A Cost-Effective High-Efficiency Power Conditioner With Simple MPPT Control Algorithm for Wind-Power Grid Integration

Katsumi Nishida, *Member, IEEE*, Tarek Ahmed, *Member, IEEE*, and Mutsuo Nakaoka, *Member, IEEE*

***Abstract*—In this paper, a novel grid integration system for a variable-speed wind turbine using an interior permanent-magnet synchronous generator (IPMSG) is developed. The power conditioner system (PCS) consists of a series-type 12-pulse uncontrolled diode rectifier powered by a phase-shifting transformer and then cascaded to a pulsewidth-modulated (PWM) voltage source inverter. The active current of the grid-side PWM inverter is only controlled to follow the optimal active current reference which is determined by using a simple maximum power point tracking (MPPT) control strategy. The MPPT algorithm requires only three sensors in order to track the maximum power of the wind turbine. The most significant advantage of the proposed system is that the passive filter together with a series-type 12-pulse rectifier provides high efficiency by compensating the power factor angle of the IPMSG and suppresses distortions presented in the IPMSG voltages and currents. The laboratory results indicate that the proposed construction and scheme are simple, cheap, and efficient.**

***Index Terms*—Grid integration, interior permanent-magnet synchronous generator (IPMSG), maximum power point tracking (MPPT) control strategy, power conditioner system (PCS), wind turbine.**

I. Introduction

OPERATION at an optimum speed in response to wind velocity minimizes fluctuations of power output and their effects on the power grid. Compared with conventional wind turbines, many improvements are required in performance and reliability to achieve higher economic efficiency and to promote the introduction of wind-power generation [1]–[3]. Consequently, large-scale wind turbines employing pitch control, variable-speed control, and a permanent-magnet synchronous generator are increasingly viable. It is concluded from previous research that a combination of a permanent-magnet synchronous generator and an inverter/converter has allowed fluctuations of wind-turbine output and voltage variation to be greatly reduced. Furthermore, there is no rush current when the generator is incorporated into the power grid system [4]–[6]. Although a maximum power point tracking (MPPT) control can be realized and the generator efficiency can be easily kept at the maximum value, this system is expensive [7]–[10].

In terms of the use of the synchronous generator, a simple alternative scheme is used when the generator-side converter is replaced by a three-phase diode rectifier and a chopper [11]–[15]. This scheme is low cost when compared with the full-power converter. When the speed of the generator alters, the voltage value on the dc side of the diode rectifier will change. A step-up chopper is used to adapt the rectifier voltage to the dc-link voltage of the inverter [10]. The step-up chopper used as a rectifier utilizes a high switching frequency, implying that the bandwidth of these components is much higher than the bandwidth of the generator. Controlling the inductance current in the step-up chopper can control the machine torque and, therefore, its speed. However, this method generates high voltage surges on the generator windings and thus reduces the life span of the generator particularly with a high-power wind-turbine system. In [14], a buck–boost converter is proposed for a dc–dc chopper and the output current reference of the chopper is designed for the MPPT control of the wind turbine. However, the voltage stress of the chopper switch is greater than that of the boost converter. In addition, the leakage inductance of the generator and cable cannot be used as an equivalent dc inductor.

In this paper, a power conditioner system (PCS) consisting of a series-type 12-pulse rectifier and a three-phase voltage-fed PWM inverter with a simple MPPT control strategy for wind-power grid integration of the interior permanent-magnet synchronous generator (IPMSG) is developed. The losses in the IPMSG can be effectively reduced by setting a passive filter at the generator terminals, and the grid-side PWM inverter is able to supply sinusoidal currents to the power grid within a wide range of the system speed operation. The power factor of the grid-side PWM inverter can be adjusted by controlling its reactive current control. However, the reference for the active current of the grid-side inverter is set for the MPPT of the wind turbine by a simple proposed algorithm. The results of a 1.5-kW system indicate that the construction and installation are simple and reliable.

II. System Description

Fig. 1 shows the conventional scheme of the full-power converters [1]–[3] while Fig. 2 shows the schematic diagram of

Manuscript received March 25, 2010; revised June 29, 2010; accepted September 27, 2010. Date of publication December 30, 2010; date of current version March 18, 2011. Paper 2010-IPCC-111.R1, presented at the 2009 International Conference on Power Electronics and Drive Systems, Taipei, Taiwan, November 2–5, and approved for publication in the IEEE TRANSACTIONS ON INDUSTRY APPLICATIONS by the Industrial Power Converter Committee of the IEEE Industry Applications Society.

K. Nishida is with Ube National College of Technology, Ube 755-8555, Japan (e-mail: nishida5@bronze.ocn.ne.jp).

T. Ahmed is with Assiut University, Assiut 71515, Egypt (e-mail: TarekAhmed@ieee.org).

M. Nakaoka is with The Electric Energy Saving Research Center, Kyungnam University, Masan 631-701, Korea (e-mail: nakaoka@pe-news1.eee.yamaguchi-u.ac.jp).

Color versions of one or more of the figures in this paper are available online at http://ieeexplore.ieee.org.

Digital Object Identifier 10.1109/TIA.2010.2103294

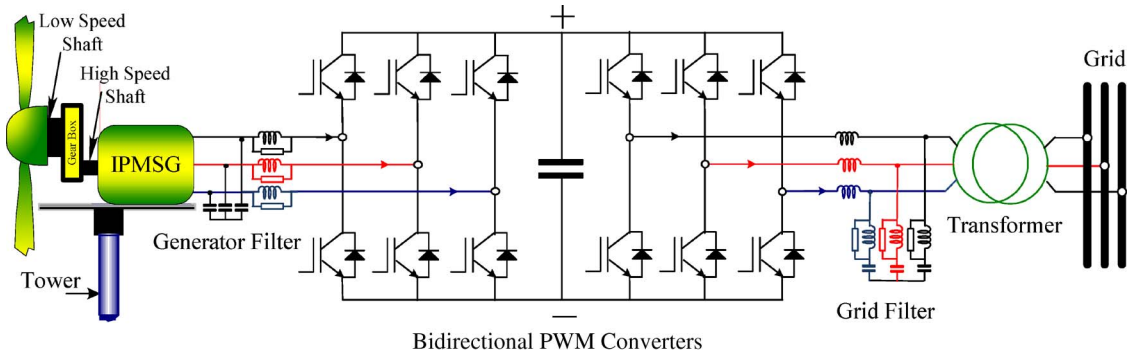

Fig. 1. Conventional system of full-power converter for a wind-turbine-driven IPMSG.

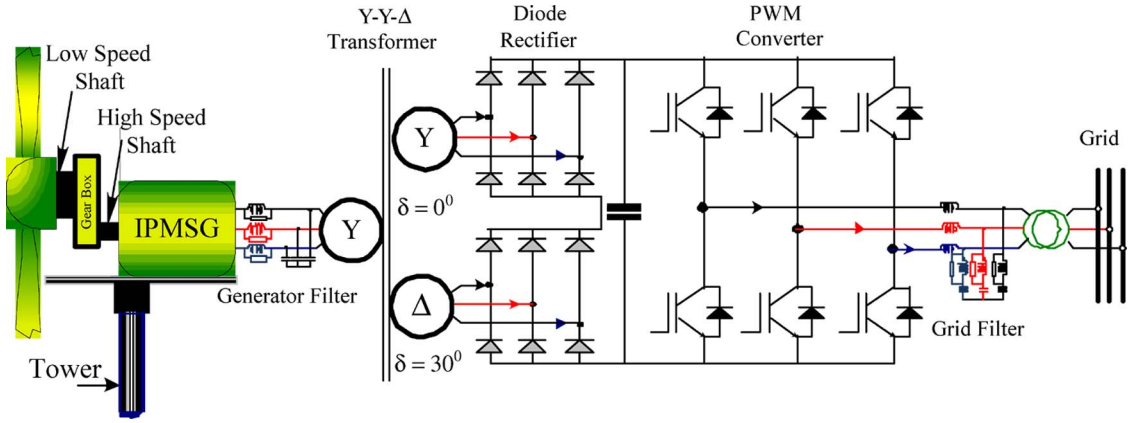

Fig. 2. Series-type 12-pulse rectifier and a PWM inverter for wind-power generation system.

the proposed wind-power generation system. In Fig. 2, a PCS consisting of a series-type 12-pulse rectifier and a three-phase voltage-fed PWM inverter with a simple proposed MPPT control algorithm for wind-power grid integration of the IPMSG is illustrated. The weight of the transformer utilized on the generator-side 12-pulse diode rectifier may be heavy because of the low-frequency operation of the generator power output. However, it is not a big issue since the PCS can be installed on the onshore site of the wind turbine when connecting the turbine to the ac system. The proposed configuration has advantages in terms of low cost and high reliability compared with the conventional system, as shown in Fig. 1. To realize the high-efficiency operation of the generator which can be achieved by connecting a simple passive filter at the generator terminal, the accurate design of the passive LC filter for optimum parameters should compensate the power factor angle of the generator.

In addition, owing to employing not a parallel but a series-type 12-pulse rectifier, the dc-link voltage can be easily kept at a high value enough to operate the latter utility-connected inverter even in a low-speed area.

A. Design Method of the Passive Filter

Table I indicates the specification parameters of the IPMSG used in experiments. The passive filters, set at the generator terminals as shown in Fig. 2, are designed not only to decrease harmonic voltages and currents observed at the terminals of the generator but also to improve the generator efficiency. To minimize the total losses in the stator windings and iron core of

TABLE I
SPECIFICATIONS OF THE 1.5-kW IPMSG

Symbol	Quantity	Number
ϕa	Magnet flux -linkage	0.235 Wb
p	number of pole pairs	3
Lq	q-axis inductance	11.96 mH
Ld	d-axis inductance	8.90 mH
Ra	Armature resistance	0.774Ω
Iam	Maximum current	6.3 A
Rc	Iron Loss Resistance	444.6 Ω

the generator, the desired weakening exciting stator current i_{gd}^* of the permanent-magnet flux with an indefinite q-axis stator current i_{gq}^* is given by [16]

$$i_{gd}* = \frac{\sqrt{1.5}\phi_a}{2(L_q - L_d)} \frac{R_a + b \cdot (2-\gamma)}{R_a + b} - \sqrt{\frac{1.5\phi_a^2}{4(L_q - L_d)^2} \cdot \left(\frac{R_a + b\cdot\gamma}{R_a + b}\right)^2 + {i_{gq}^*}^2 \cdot \frac{R_a + b\cdot\gamma^2}{R_a + b}} \quad (1)$$

where $b = (\omega L_d)^2/R_c$ and $\gamma = L_q/L_d$.

Then, the desired current phase θ^* on the d–q frame, the angle between the back-induced emf $\boldsymbol{e}$ and the current $\boldsymbol{i_g}$ of the IPMSG, for achieving the high-efficiency operation of the generator through decreasing the copper and iron losses is set by

$$\theta* = \tan^{-1}\left(\frac{-i_{gd}^*}{i_{gq}*}\right). \quad (2)$$

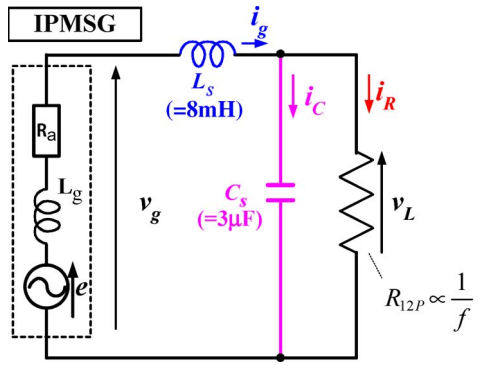

Fig. 3. Simplified equivalent circuit of IPMSG with filter and rectifier.

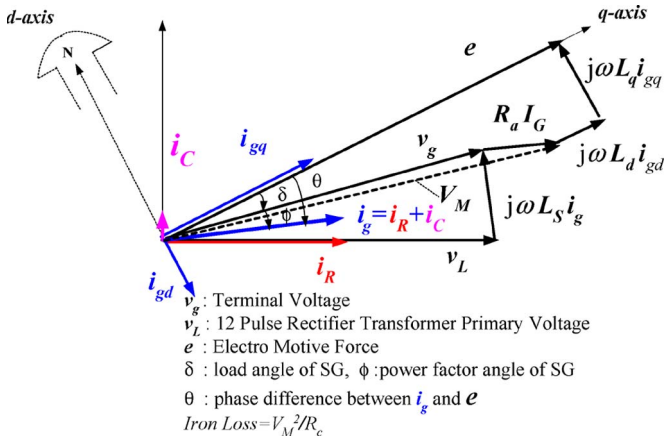

Fig. 4. Vector diagram of the IPMSG in steady state.

Figs. 3 and 4 show the simplified equivalent circuit of the proposed system and its vector diagram, respectively, to obtain the angle θ. In Fig. 3, the passive filter is represented by L_s and C_s and the 12-pulse rectifier is modeled by a resistance R_{12P}, which is inversely proportional to the generator frequency. The angle θ can be determined by the following, which is based on Fig. 4:

$$\theta = \phi + \delta \tag{3}$$

where ϕ is the power factor angle and δ is the load angle. Moreover, ϕ and δ can be estimated as follows:

$$\phi = \tan^{-1}\left(\frac{2\pi f L_s + (2\pi f)^3 L_s \cdot C_s^2 \cdot R_{12P}^2 - 2\pi f C_s \cdot R_{12P}^2}{R_{12P}}\right) \tag{4}$$

$$P_G = \frac{e \cdot v_g}{2\pi f L_d} \cdot \sin\delta - \frac{v_g^2 (L_q - L_d)\sin 2\delta}{2 \cdot 2\pi f \cdot L_q L_d} + v_g R_a i_g \left\{\frac{\cos\delta \cdot \sin(\phi+\delta)}{2\pi f L_q} - \frac{\cos(\phi+\delta)\cdot\sin\delta}{2\pi f L_d}\right\} \tag{5}$$

where P_G is the generator power output.

Calculation example: f = 70 Hz, desired $P_G = 560$ W, $L_s = 8$ mH, $C_s = 3$ μF, $v_g = 118$ V (experimental result) → $R_{12P} \cong v_g^2/P_G = 24.9\ \Omega$, $\phi = 9.2°$, $i_g = 4.81$ A, $\delta = 10.8°$ (measured value : $\phi = 9.2°$, $i_g = 4.76$ A, $\delta = 10.8°$), while $\theta^* = 19.9°$.

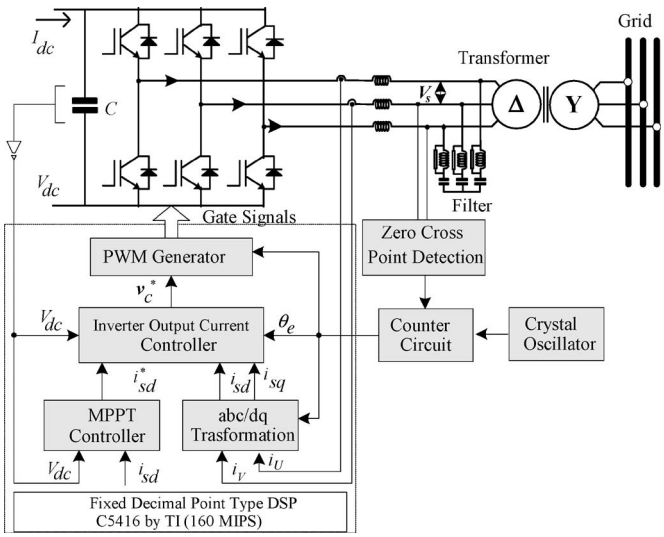

Fig. 5. Circuit and control diagram of MPPT control algorithm for grid-side PWM inverter.

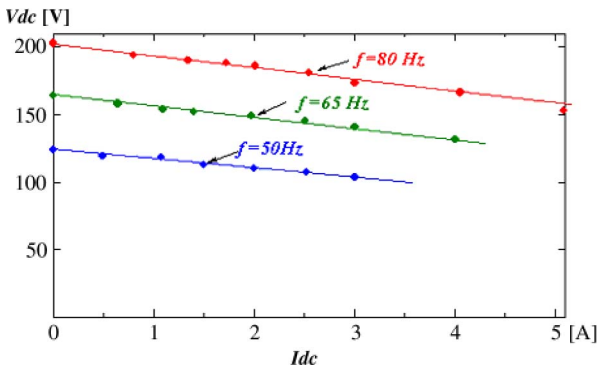

Fig. 6. Linear characteristics of IPMSG with series-type 12-pulse rectifier.

B. Estimation Method of the Generator Frequency

The three-phase voltage-fed PWM inverter is connected to the power grid through three-phase transformers, as shown in Fig. 5. Fig. 6 shows the experimental results of the dc-link voltage of the series-type 12-pulse rectifier under the conditions of dc load and speed variations. The results indicate that the relation between the dc-link voltage and current is linear and is given experimentally as follows:

$$V_{\mathrm{dc0}} = V_{\mathrm{dc}} + k \cdot I_{\mathrm{dc}} \tag{6}$$

where V_{dc} is the measured dc-link voltage of the series-type 12-pulse rectifier, V_{dc0} is the dc-link voltage at the no-load condition, I_{dc} is the dc-link current, and k ($k = 8.0$ V/A) is a constant. Based on the experimental results represented by (6), the dc-link voltage V_{dc0}, which is required to determine the generator frequency f, is estimated using both the measured dc-link voltage V_{dc} and the dc-link current I_{dc}.

By making the power balance between the dc-link power and the power supplied to the grid with neglecting the power losses

in the grid-side PWM inverter, the dc-link current $I_{\rm dc}$ can be calculated as follows:

$$I_{\rm dc} = \frac{V_s}{V_{\rm dc}} i_{\rm sd}. \tag{7}$$

Therefore, $V_{\rm dc0}$ can be redefined by substituting (7) in (6) as follows:

$$V_{\rm dc0} = V_{\rm dc} + k \cdot V_s \cdot i_{\rm sd}/V_{\rm dc} \tag{8}$$

where $i_{\rm sd}$ is the measured active current of the inverter and V_s is the rms value of line voltage ($= 50$ V).

On the other hand, $V_{\rm dc0}$ can be also calculated from the steady-state characteristic equation of the IPMSG as follows.

The maximum value of the generator phase voltage E_M is given by

$$E_M = 2\pi f \cdot \phi_a \tag{9}$$

while the maximum value of the secondary line-to-line voltage of the transformer V_{2M} is defined by

$$V_{2M} = E_M \times \frac{1}{n} \times \sqrt{3} \tag{10}$$

where ϕ_a is the maximum flux linkage due to the permanent magnet per phase ($\phi_a = 0.235$ Wb) and n is the turn ratio of the transformer. As the rectifier is a series 12-pulse type with deviation angle of 30°, V_{dc0} can be also calculated from

$$\begin{aligned} V_{\rm dc0} &= |\dot{V}_{2M} + \dot{V}_{2M} e^{j\delta}| = V_{2M} \cdot 2 \cdot \cos 15^0 \\ &= 2\pi f \phi_a \times \frac{1}{n} \times \sqrt{3} \times 2 \times \cos 15^0 = 2.47 \times f. \end{aligned} \tag{11}$$

Finally, the generator frequency is defined by using (8) and (11) as follows:

$$f = \frac{V_{\rm dc} + k \cdot V_s \cdot i_{\rm sd}/V_{\rm dc}}{2.47}. \tag{12}$$

C. MPPT Control for PWM Inverter

The current reference $i^*_{\rm sd}$ of the grid-side converter is calculated from the predetermined maximum output power of the wind turbine according to the generator frequency which is defined by

$$P_{\rm Turbine} = K_{\rm opt} \cdot f^3. \tag{13}$$

By neglecting the power loss and making the power balance between the optimum output power of the turbine defined by (13) and the power supplied to the grid, the active current reference $i^*_{\rm sd}$ of the grid-side inverter is defined as

$$i^*_{\rm sd} = \frac{K_{\rm opt}}{V_s} f^3 \tag{14}$$

where $K_{\rm opt}$ is a constant and reflects the characteristics of the wind turbine. $K_{\rm opt}$ is given by

$$K_{\rm opt} = \frac{1}{2} \rho \pi R^2 C_{\rm opt} \eta_g \eta_b \left(\frac{2\pi R}{p \lambda_{\rm opt}} \right)^3 \tag{15}$$

where $C_{\rm opt}$ is the maximum power coefficient, $\lambda_{\rm opt}$ is the optimum tip speed ratio, ρ is the air density (in kilograms per cubic meter), R is the turbine radius (in meters), η_g is the generator efficiency, η_b is the gearbox/bearings efficiency, and p is the number of pair poles of the generator.

When the losses in the proposed system are considered, $i^*_{\rm sd}$ can be easily set by using a lookup table in the DSP program. Based on the aforementioned principle, the control block diagram of the inverter is constructed, as shown in Fig. 5. The current reference is set to achieve the desired MPPT scheme which results in the maximum active power being supplied to the grid from the wind turbine with a unity power factor. The current controller has fast a response as it works in a synchronous reference frame.

III. Experimental Results

The appropriate design of the passive filter without increasing the generator current constitutes a simple solution for not only providing a good operating waveform performance dealing with the series-type 12-pulse rectifier as a harmonics source but also improving the generator efficiency.

Fig. 2 is used to implement the system in the laboratory to demonstrate the functions of the passive filter and investigate the significant advantage of the proposed MPPT algorithm which has been applied and tested for a 1.5-kW IPMSG prototype setup. The parameters of the proposed system are listed in Table I.

A. Effect of the Designed Passive Filter

The operating waveforms of the IPMSG system in terms of the IPMSG terminal voltage v_{gAB}, the IPMSG stator current i_{gA}, the grid line-to-line voltage v_{VW}, and the grid-side inverter current i_U are shown in Fig. 7(a) and (b). The operating waveforms are highly distorted if the passive filter is not used. Fig. 7(a) shows that the harmonic distortion observed at the generator current is 7.4% while the harmonic distortion of the generator voltages is 10.4%. These harmonic distortions exceed the acceptable limits suitable for the high operating performance of the generator.

When the passive filter, represented by $L_s = 8$ mH and $C_s = 1$ μF in delta connection, is used together with a series-type 12-pulse rectifier, the harmonic distortion observed at the generator current is reduced from 7.4% to 3.4%. At the same time, the harmonic distortion of the generator voltages is reduced from 10.4% to 4.6%. Such reductions can be observed in Fig. 7(b). The series-type 12-pulse rectifier powered by a phase-shifting transformer with the designed passive filter shows its ability to reduce the total harmonic distortion (THD) of the generator. It is possible to see that the grid currents and voltages have a good operating waveform performance. The THD of the grid currents is less than 1.1%, while the THD of the grid voltages 2.6%.

B. Effect of the Designed Passive Filter With Different Generator Frequencies

In Fig. 8, it is possible to see the generator speed/frequency effect on the generator current waveforms when the designed

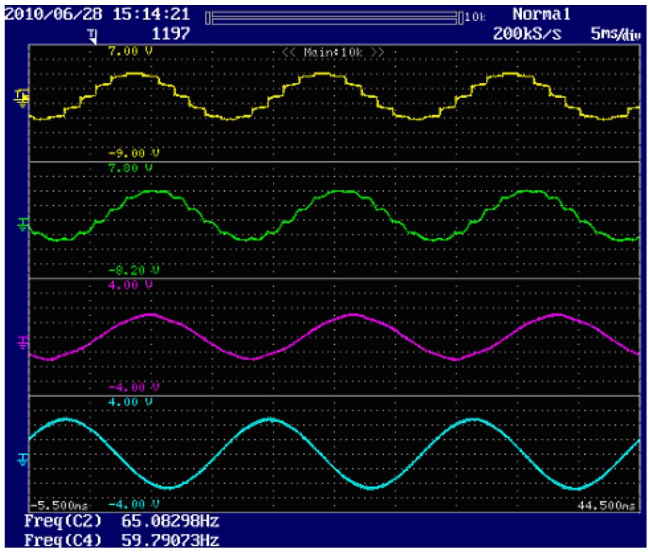

Ch-1: IPMSG terminal voltage v_{gAB} -100 *V/div.*, 65.1Hz, THD=10.4%
Ch-2: IPMSG stator current i_{gA} - 2 *A/div.*, THD=7.4%
Ch-3: Grid voltage v_{VW} −50 *V/div.*, THD=2.6%
Ch-4 Grid-side inverter current i_U − 2.5 *A/div.*, THD=1.1%
(a)

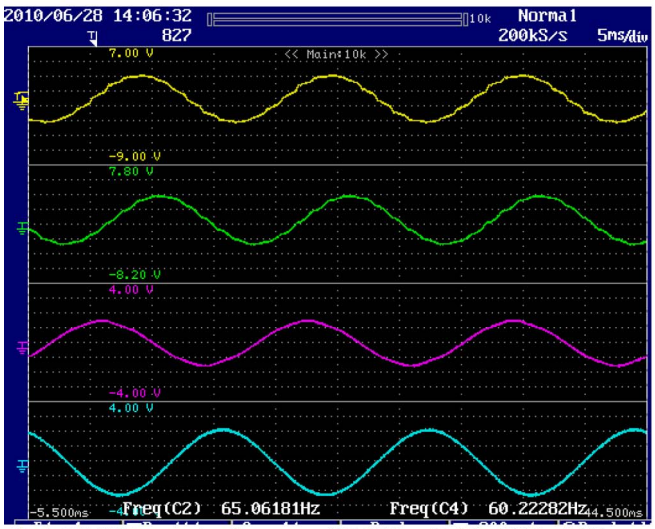

Ch-1: IPMSG terminal voltage v_{gAB} -100 *V/div.*, 65.1Hz, THD=4.6%
Ch-2: IPMSG stator current i_{gA} - 2 *A/div.*, THD=3.4%
Ch-3: Grid voltage v_{VW} - 50 *V/div.*, THD=2.2%
Ch-4 Grid-side inverter current i_U - 2.5 *A/div.*, THD=0.8%
(b)

Fig. 7. Operating waveforms of the IPMSG system. (a) Passive filter is not connected. (b) Passive filter is connected.

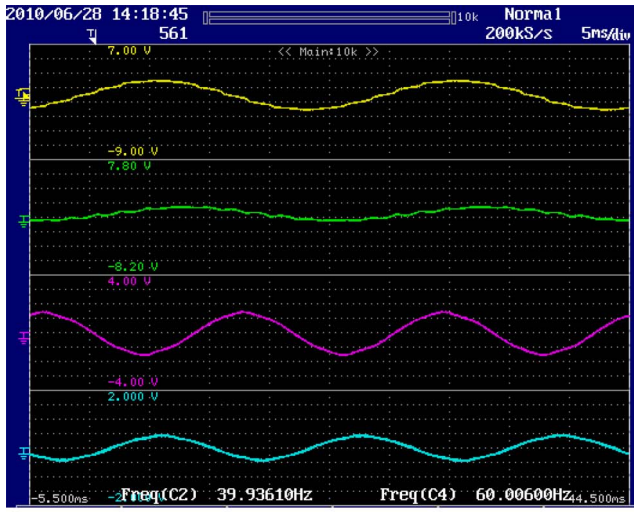

Ch-1: IPMSG terminal voltage v_{gAB} -100 *V/div.*
Ch-2: IPMSG stator current i_{gA} - 2 *A/div.*
Ch-3: Grid voltage v_{VW} - 50 *V/div.*
Ch-4 Grid-side inverter current i_U − 1.25 *A/div.*
(a)

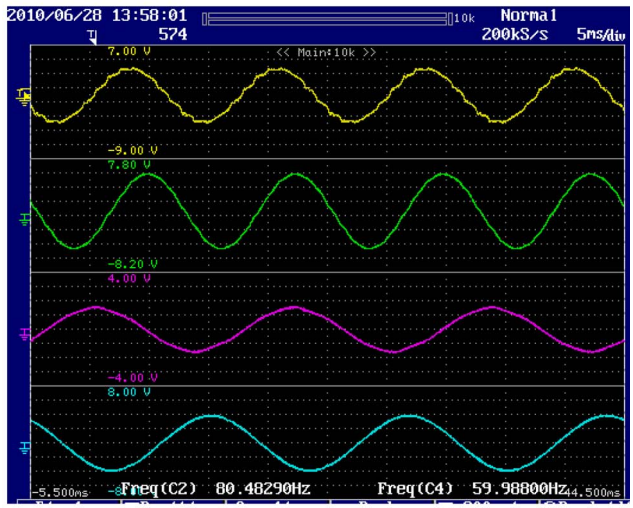

Ch-1: IPMSG terminal voltage v_{gAB} -100 *V/div*
Ch-2: IPMSG stator current i_{gA} - 2 *A/div.*
Ch-3: Grid voltage v_{VW} - 50 *V/div.*
Ch-4 Grid-side inverter current i_U - 5 *A/div.*
(b)

Fig. 8. Operating waveforms of the IPMSG system with different output frequencies. (a) Generator $f = 40.0$ Hz (THD of $v_{gAB} = 4.5\%$ and THD of $i_{gA} = 12\%$). (b) Generator frequency $f = 80.3$ Hz (THD of $v_{gAB} = 5.0\%$ and THD of $i_{gA} = 1.8\%$).

passive filter is connected. The harmonic distortion contents at the generator voltage are reduced to 4.5% with 40.0 Hz and 5.0% with 80.3 Hz.

Fig. 9 shows that the designed passive filter, as illustrated in Fig. 3, can provide rather good phase compensation performances in order to minimize the total losses of the generator, which consists of the copper loss in the stator winding and the iron loss in the stator core.

Fig. 10 shows the measurements of the d- and q-axis stator current components of the generator under a wide frequency operation range. In addition, Fig. 10 shows the stator flux of the generator which can be derived by using the following:

$$\text{StatorFlux} = \sqrt{(\phi_{\text{a}} + \text{L}_{\text{d}} \cdot \text{i}_{\text{gd}}/\sqrt{1.5})^2 + (\text{L}_{\text{q}} \cdot \text{i}_{\text{gq}}/\sqrt{1.5})^2}. \tag{16}$$

Fig. 10 shows that the actual stator flux of the generator is less than the permanent-magnet flux during the whole generator speed range. Therefore, the flux saturation is not observed.

Fig. 11 compares the efficiency of the IPMSG having a passive filter connected at the ac side of the series-type 12-pulse rectifier with that of the IPMSG which uses the PWM rectifier. By minimizing the total losses of the IPMSG through the PWM rectifier, it is found that the passive filter, as a low-cost solution, provides a similar efficiency compared with that of the

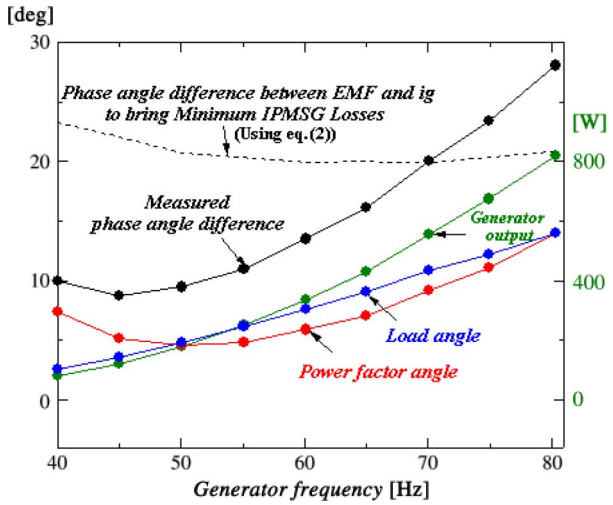

Fig. 9. Phase compensation performance of the proposed passive filter.

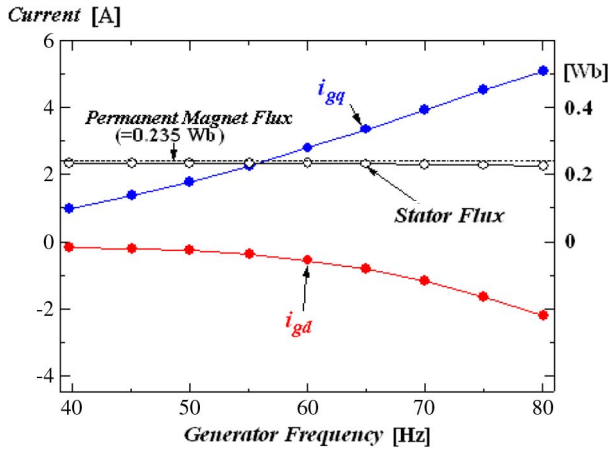

Fig. 10. Measured stator flux with d- and q-axis current components of the IPMSG under a wide frequency operation range.

high-cost one, because the compensation of the power factor angle is made by the passive filter, as shown in Fig. 9.

C. Effect of the Proposed MPPT Control Strategy

Fig. 12 shows the dynamic responses of the measured active and reactive currents of the PWM inverter with speed variations. The reference for the q-axis or reactive current is set to zero for unity power factor operation, while the d-axis or active current and the active power are supplied to the power grid based on the MPPT control strategy. As the q-axis current is controlled to be zero, the peak envelop of phase current i_U is 0.816 times the magnitude of the d-axis current and the power factor control is possible for the reactive power control. It also keeps the THD as low as possible, thus improving the power quality supplied to the grid.

Fig. 13 shows the estimated frequency error of the proposed MPPT control strategy in steady state, for a wide range of operating frequency. The results indicate that the estimated error of the generator frequency using the proposed MPPT control method is less than 2.8%.

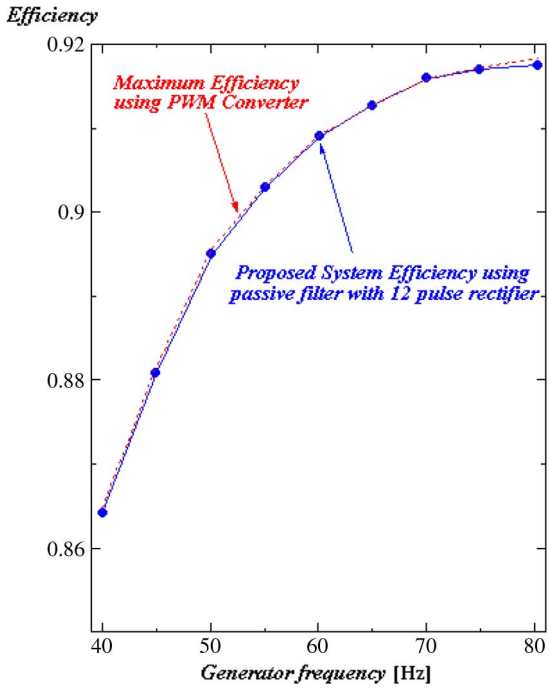

Fig. 11. Comparison in efficiency between the IPMSG with a passive filter and the IPMSG with the PWM rectifier.

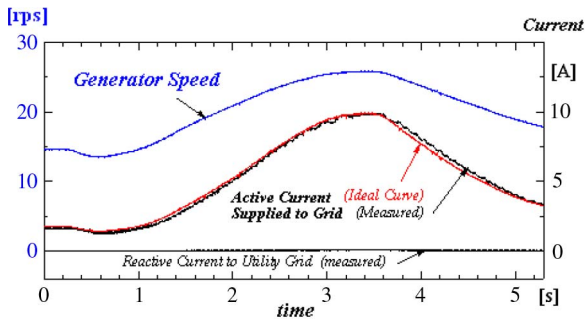

Fig. 12. Measured active and reactive current components of the grid-side inverter in dynamic response.

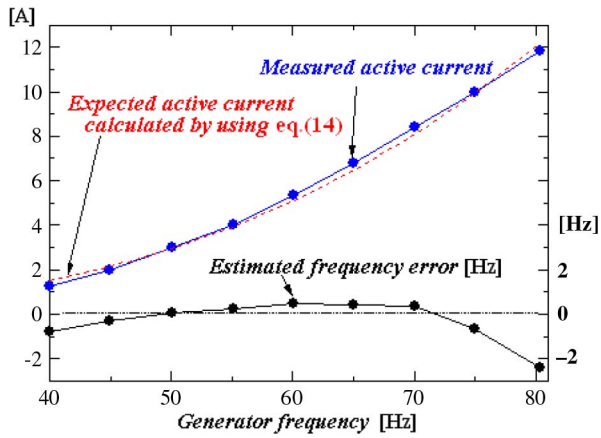

Fig. 13. Measured and reference active currents of the grid-side PWM inverter with estimated frequency error of the proposed MPPT control method.

Fig. 13 also shows the measured and expected active currents of the PWM inverter with the proposed MPPT control method in comparison with the generator frequency in a wide frequency

operation range. As the generator frequency changes from 40 to 80 Hz, the reference current changes accordingly in order to maximize the wind-power output calculated from (14). The active current of the grid-side PWM inverter is adjusted within a 3.0% error in order to achieve the proposed MPPT control strategy.

The results of the proposed system indicate that the construction and installation are simple, reliable, and efficient. Moreover, the IPMSG losses can be reduced as the designed passive filter draws a lag current in proportion to the square of the generator frequency.

IV. Conclusion

In this paper, a novel and simple MPPT control algorithm for a grid-side PWM inverter cascaded in series with a series-type 12-pulse rectifier for a variable-speed wind-power generation system has been proposed. The wind speed and/or generator speed is measured from the rectified output voltage of the IPMSG, and the maximum output power is supplied to the grid. Therefore, the proposed control algorithm does not require any speed sensor for measuring the wind speed or the mechanical IPMSG speed. As the proposed system requires only one PWM inverter to attain the MPPT control, the system cost can be reduced and high reliability can be achieved. The power factor of the grid-side inverter can be kept at unity. Moreover, the designed passive filter connected at the terminal of the IPMSG reduces the harmonic distortion observed in the line current and the terminal voltage of the generator. The function of the passive filter is not only the harmonic elimination but also the reduction of the total losses of the generator.

The laboratory results from the implementation of the simple ac–dc–ac power conversion circuit employed with the MPPT control algorithm indicate that the proposed system has advantages. These include high reliability, cost effectiveness, and a wide speed range for variable-speed wind-turbine controllers.

References

[1] S. Heier, *Grid Integration of Wind Energy Conversion Systems*. Hoboken, NJ: Wiley, 1998.

[2] M. Tazil, V. Kumar, R. C. Bansal, S. Kong, Z. Y. Dong, W. Freitas, and H. D. Mathur, "Three-phase doubly fed induction generators: An overview," *IET Elect. Power Appl.*, vol. 4, no. 2, pp. 75–89, Feb. 2010.

[3] J. Ribrant and L. M. Bertling, "Survey of failures in wind power systems with focus on Swedish wind power plants during 1997–2005," *IEEE Trans. Energy Convers.*, vol. 22, no. 1, pp. 167–173, Mar. 2007.

[4] N. A. Cutululis, E. Ceanga, A. D. Hansen, and P. Sørensen, "Robust multi-model control of an autonomous wind power system," *Wind Energy*, vol. 9, no. 5, pp. 399–419, Sep./Oct. 2006.

[5] R. Pena, J. C. Clare, and G. M. Asher, "Doubly fed induction generator using back-to-back PWM converters and its application to variable-speed wind-energy generation," *Proc. Inst. Elect. Eng.—Elect. Power Appl.*, vol. 143, no. 3, pp. 231–241, Feb. 1996.

[6] S. Morimoto, T. Nakamura, and Y. Takeda, "Power maximization control of variable speed wind generation system using permanent magnet synchronous generator," *IEEJ Trans. Power Energy*, vol. 123-B, no. 12, pp. 1573–1579, 2003.

[7] K. Nishida, T. Ahmed, and M. Nakaoka, "Induction generator hybrid applications with active power filter," *Proc. Inst. Elect. Eng.—Elect. Power Appl.*, vol. 153, no. 2, pp. 197–205, Mar. 2006.

[8] T. Ahmed, K. Nishida, and M. Nakaoka, "Advanced control of PWM converter with variable speed induction generator," *IEEE Trans. Ind. Appl.*, vol. 42, no. 4, pp. 934–945, Jul./Aug. 2006.

[9] T. F. Chan, W. Wang, and L. L. Lai, "Analysis and performance of a permanent-magnet synchronous generator supplying an isolated load," *IET Elect. Power Appl.*, vol. 4, no. 3, pp. 169–176, Mar. 2010.

[10] L. Grzesiak, W. Koczara, and M. da Ponte, "Application of a permanent magnet machine in the novel hygen adjustable speed load-adaptive electricity generating system," in *Proc. Int. Conf. IEMD*, 1999, pp. 398–400.

[11] K. Tan and S. Islam, "Optimum control strategies in energy conversion of PMSG wind turbine system without mechanical sensors," *IEEE Trans. Energy Convers.*, vol. 19, no. 2, pp. 392–399, Jun. 2004.

[12] S. Jiao, G. Hunter, V. Ramsden, and D. Patterson, "Control system design for a 20 kW wind turbine generator with a boost converter and battery bank load," in *Proc. IEEE 32nd Annu. PESC*, 2001, vol. 4, pp. 2203–2206.

[13] S. Song, S. Kang, and N. Hahm, "Implementation and control of grid connected AC–DC–AC power converter for variable speed wind energy conversion system," in *Proc. 18th Annu. IEEE APEC*, 2003, vol. 1, pp. 154–158.

[14] Y. Higuchi, N. Yamamura, M. Ishida, and T. Hori, "An improvement of performance for small-scaled wind power generating system with permanent magnet type synchronous generator," in *Proc. 26th IEEE IECON*, 2000, vol. 2, pp. 1037–1043.

[15] R. Hoffmann and P. Mutschler, "The influence of control strategies on the energy capture of wind turbines," in *Conf. Rec. IEEE IAS Annu. Meeting*, 2000, pp. 886–893.

[16] C. Mademlis and N. Margaris, "Loss minimization in vector-controlled interior permanent-magnet synchronous motor drives," *IEEE Trans. Ind. Electron.*, vol. 49, no. 6, pp. 1344–1347, Dec. 2002.

Katsumi Nishida (M'05) was born in Yamaguchi, Japan, in 1954. He received the B.S. and M.S. degrees in electrical engineering from Tokyo Institute of Technology, Tokyo, Japan, in 1976 and 1978, respectively, and the Ph.D. degree in electrical engineering from Yamaguchi University, Ube, Japan, in 2002.

He is currently a Professor in the Department of Electrical Engineering, Ube National College of Technology, Ube. His research interests are in the design and control of power conditioners with deadbeat technique and adaptive signal processing technique.

Dr. Nishida is a member of the Institute of Electrical Engineers of Japan, the Power Electronics Society of Japan, and the Institute of Installation Engineers of Japan. He was the recipient of the Best Paper Award at the 8th IEEE International Conference on Power Electronics and Drive Systems in 2009.

Tarek Ahmed (S'03–M'06) received the Ph.D. degree in electrical engineering from Yamaguchi University, Ube, Japan, in 2006.

He conducted research within the Renewable Energy Research Group, University of Exeter, Exeter, U.K., in the area of wave energy development to create a major grid-connected project off the north coast of Cornwall, U.K., in 2009. Currently, he is a Lecturer in the Electrical Engineering Department, Faculty of Engineering, Assiut University, Assiut, Egypt. He joined the Assiut engineering faculty in 1995 as an Instructor. In 1998, upon completion of his M.S. degree, he was made a Teaching Assistant in the Department of Electrical Power and Machines within the same faculty. His research interests are in power electronics and electric machine control for grid integration of renewable energy.

Dr. Ahmed was the recipient of Best Paper Awards from the Institute of Electrical Engineers of Japan in 2003, 2004, and 2005, Best Paper and Student Awards at the 30th Annual Conference of the IEEE Industrial Electronics Society in 2004, the Best Paper Award at the International Conference on Electrical Machines and Systems in 2004, and the Best Paper Award at the 8th IEEE International Conference on Power Electronics and Drive Systems in 2009.

Mutsuo Nakaoka (M'83) received the Ph.D. degree in electrical engineering from Osaka University, Suita, Japan, in 1981.

He joined the Department of Electrical and Electronics Engineering, Kobe University, Kobe, Japan, in 1981. Since 1995, he had been a Professor in the Graduate School of Science and Engineering, Yamaguchi University, Ube, Japan. He is currently a Visiting Professor at the Electrical Energy Saving Research Center, Kyungnam University, Masan, Korea. His research interests include state-of-the-art power electronics circuits and systems engineering.

Dr. Nakaoka is a member of the Institute of Electrical Engineers of Japan, The Institute of Electronics, Information, and Communication Engineers of Japan, The Illuminating Engineering Institute of Japan, the Power Electronics Society of Japan, and the Institute of Installation Engineers of Japan. He has been the recipient of many distinguished paper awards, including the 2001 Premium Prize Paper Award from the Institution of Electrical Engineers, U.K., the 2001/2003 IEEE IECON Best Paper Award, the Third Paper Award at the 2000 IEEE International Conference on Power Electronics and Drive Systems, the 2003 IEEE-IAS James Melcher Prize Paper Award, the Best Paper Award at Industry Appliance Technical Conference 2006, the IEEE-PEDS 2009 Best Paper Award, and the IEEE-ISIE 2009 Best Paper Award. From 2001 to 2006, he served as the Chairman of the IEEE Industrial Electronics Society Japan Chapter.